

Robust sensorless predictive control of induction motors with sliding mode voltage model observer

Seyed Alireza DAVARI,^{1,*} Davood Arab KHABURI,¹ Fengxiang WANG,² Ralph KENNEL²

¹Center of Excellence for Power Systems Automation and Operation, Electrical Engineering Department, Iran University of Science and Technology, Tehran, Iran

²Institute for Electronics Drive Systems & Power Electronics, Technical University of Munich, Munich, Germany

Received: 03.10.2011 • Accepted: 23.05.2012 • Published Online: 02.10.2013 • Printed: 28.10.2013

Abstract: In this paper, a robust sliding mode prediction model is combined with a sliding mode voltage model observer to achieve a sensorless predictive torque control method. In order to compensate the uncertainties of the stator and rotor resistances and the offset of measured current, sliding mode feedbacks were added to the voltage model observer. To reduce the effect of the errors that are injected from the observer to the prediction model in the sensorless application, the prediction model was also reinforced by a sliding mode feedback. The feedback gains for the prediction and observer models are assigned by a robustness H_∞ analysis. This method reduces the sensitivity of the sensorless predictive algorithm to the parameter variation. In order to verify the proposed method, simulation and experimental results are presented in a wide speed range.

Key words: Predictive torque control, robust sensorless drive, induction motor, observer, sliding mode

1. Introduction

The predictive torque control (PTC) method was introduced to overcome the problems of the direct torque control (DTC) method, e.g., high torque ripple and variable switching frequency. However, the speed sensor has been utilized in most kinds of PTC methods that were investigated to date. This is a dominant disadvantage compared to the DTC method. The different kinds of PTC methods will be briefly reviewed below.

Direct mean torque control controls the mean value of the torque by means of predicting the slope of the torque [1–3]. The deadbeat method calculates the voltage reference, which will direct the motor to produce torque and flux references [4]. If a cost function, which is a function of errors of control variables, is minimized, this method is known as model predictive control (MPC) [5]. A special kind of MPC is generalized predictive control, in which the minimization method is based on a CARIMA model [5–7]. There is another approach for the cost function minimization. Finite control set-model predictive control (FCS-MPC) examines all feasible voltage vectors (VVs) in the cost function. The VV that minimizes the cost function is selected [8–12].

Since accurate prediction in all kinds of predictive methods is necessary, a speed dependent full order model of the induction motor is used for prediction. This model is known as a prediction model. In order to perform an accurate prediction, the measured speed has been mostly used in the prediction model to date. Furthermore, accuracy of the observer affects the prediction accuracy because the outputs of the observer are used in the prediction model. Therefore, in a sensorless predictive method there are 2 problems to be considered:

*Correspondence: adavari@iust.ac.ir

- 1) Accurate prediction of the torque and flux without measuring the speed.
- 2) Accurate estimation of the torque, flux, and speed without using the measured speed.

There have been few investigations to implement PTC without using the speed sensor. In [13], a sensorless deadbeat control was proposed. Though the full order observer was utilized, because of the weak robustness of the deadbeat method [14], this method was not reliable for the sensorless application. Saliency based sensorless PTC method was used for the reluctance motor in [15]. The problem of parameter sensitivity was solved by means of the techniques based on the reluctance motor characteristic [16]. In [17–19], a sensorless predictive current control was used in the field oriented control (FOC) method. The speed estimation was performed by Kalman filter in [18]. The method that was introduced in [19] utilizes the reduced order observer for the flux and speed estimation and it implements a sensorless predictive current control. Though the reduced order observer has less complexity and it has a low calculation burden, it can easily be affected by the offset and parameter variation. In [20], the offset and inverter model compensation techniques were used in order to improve the performance of the sensorless PTC method. In this method, an accurate model of the inverter and a method for parameter adaptation are needed. A closed loop reduced order observer was proposed in [17] for a predictive current control in the FOC method.

In this paper, a robust closed loop sliding mode reduced order observer is used for the sensorless PTC method. Feedback gains are assigned by H_∞ analysis. Furthermore, in order to compensate the errors that are injected from the sensorless observer to the prediction model, the model is reinforced by sliding mode robust feedbacks. By using the proposed method, the sensitivity of the sensorless PTC method to the parameter variation and measurement offset is reduced and the need for parameter adaptation is eliminated. The robustness is one of the main challenges in the sensorless PTC methods because both prediction and observer models are influenced in sensorless application. The proposed method increases the accuracy of the estimation of the flux, torque, and speed, and it also decreases the sensitivity of the prediction model to the errors that are injected from the observer model.

2. Robust reduced order observer

Since the accurate prediction of the controlled states depends on the accurate estimation of the states (flux and torque) in present time, the accuracy of the observer for sensorless predictive method is critical. It should be noted that in the PTC method, the stator flux has to be estimated in addition to the speed. This is opposite to the FOC method. Therefore, the methods that are not dealt with through a model based observer, such as the methods that were introduced in [21] and [22], are not considered in this paper. Although the full order observer, which was introduced in [23] and [24], considers the full dynamic model of the motor that increases the accuracy of the model, there are 2 drawbacks when it is used in sensorless applications:

1. The full order observer is not inherently sensorless and it needs speed adaptation.
2. It increases the complexity of the control algorithm. Therefore, combination of this method with the complex control methods, such as predictive control, increases the processor's price.

Hence, if the problems of the voltage model observer are solved, it is preferred that it is used for the sensorless PTC method. The voltage model observer is a reduced order observer. It has been used as an open loop observer prevalently. Therefore, it is extremely vulnerable to parameter variation and current offset. In [20] and [25], the accurate model of the inverter, the parameter adaptation, and the offset compensation techniques are used to maintain the observer's robustness. However, the access to the accurate model of the power switches

is necessary. Besides, the parameter adaptation could cause a cumulative error. In [17], the closed loop voltage model observer is proposed and it is used for sensorless predictive control. In this paper the feedback gains of the closed loop reduced order observer are adjusted by the H_∞ method. In order to increase the robustness, a sliding mode feedback is used.

The state space equations of the induction motor in stationary frame are given by:

$$\dot{X} = A X + B U, \quad (1a)$$

$$Y = C X, \quad (1b)$$

$$X = \begin{bmatrix} \bar{\psi}_s \\ \bar{\psi}_r \end{bmatrix}, U = \bar{V}_s, Y = \bar{I}_s, \quad (1c)$$

$$A = \begin{bmatrix} -\frac{R_s}{\sigma L_s} & \frac{R_s L_m}{\sigma L_s L_r} \\ \frac{R_r L_m}{\sigma L_s L_r} & -\frac{R_r}{\sigma L_r} + j\omega_r \end{bmatrix}, \quad (1d)$$

$$B = \begin{bmatrix} I \\ 0 \end{bmatrix}, \quad (1e)$$

$$C = \begin{bmatrix} \frac{L_r}{\sigma L_s L_r} & -\frac{L_m}{\sigma L_s L_r} \end{bmatrix}, \quad (1f)$$

where $\bar{\psi}_s$ is the stator flux; \bar{V}_s and \bar{I}_s are the stator voltage and current, respectively; and R_s is the stator resistance. L_s , L_r , and L_m are the stator, rotor, and mutual inductances, respectively, and $\sigma = 1 - L_m^2/L_s L_r$. ω_r is the rotor speed.

In the voltage model observer, the first differential equation is used for speed and flux estimation. The sliding mode feedback has been proposed for the full order observer before in [24]. In this paper, this idea is proposed for the voltage model observer as below.

$$\frac{d}{dt} \hat{\psi}_s = -\frac{R_s}{\sigma L_s} \hat{\psi}_s + \frac{R_s L_m}{\sigma L_s L_r} \hat{\psi}_r + \bar{V}_s + K \operatorname{sgn}(Y - I_s) \quad (2)$$

Here, the superscript \wedge indicates the calculated variables and the variables without this superscript are measured variables.

The rotor flux should be calculated via a nondifferential equation, as follows:

$$\hat{\psi}_r = \frac{1}{L_m} \left(L_r \hat{\psi}_s - \sigma L_s L_r \bar{I}_s \right). \quad (3)$$

The synchronous speed is calculated from the rotor flux, as follows:

$$\hat{\omega}_s = \frac{d}{dt} \left(\arctan \left(\frac{\hat{\psi}_{rq}}{\hat{\psi}_{rd}} \right) \right) = \frac{\hat{\psi}_{rd}(k-1) \hat{\psi}_{rq}(k) - \hat{\psi}_{rq}(k-1) \hat{\psi}_{rd}(k)}{t_s \left| \hat{\psi}_r(k) \right|^2}, \quad (4)$$

where $\hat{\omega}_s$ is the estimated synchronous speed, k is the number of sample, and t_s is the control interval.

The rotor speed is calculated by subtracting the slip speed from the synchronous speed.

$$\hat{\omega}_r = \hat{\omega}_s - \frac{R_r \hat{T}}{\frac{3p}{4} \left| \hat{\psi}_r(k) \right|^2} \quad (5)$$

Here, $\hat{\omega}_r$ is the estimated rotor speed, R_r is the rotor resistance, p is the number of pair poles, and \hat{T} is the estimated torque, which is calculated as follows:

$$\hat{T} = \frac{3p}{4} \hat{\psi}_s \times \hat{I}_s. \quad (6)$$

In order to achieve a robust sensorless observer without parameter adaptation, feedback gains can be calculated by means of the H_∞ analysis. For the reduced order observer, the absolute error approximation method can be used [26].

$$\min_K \| G(s) - G_r(s) \|_\infty \quad (7)$$

Here, $G(s)$ and $G_r(s)$ are the transfer function of induction motor model and the reduced order closed loop observer model, respectively.

By using the balanced truncation method, which is introduced in [26], Eq. (7) can be solved by means of the following equation:

$$\| G(s) - G_r(s) \|_\infty \leq 2 \times (h_{r+1} + \dots + h_n), \quad (8)$$

where h_i is the i th Hankel singular value of the main system and r and n are the orders of the reduced order and full order model, respectively. In the case of the induction motor model and voltage model observer, $n = 2$ and $r = 1$. Since Hankel singular values of the induction motor model are speed dependent, the minimum value of h_2 among the values for a wide speed range should be used in Eq. (13). Figure 1 shows the Hankel singular values variation when the speed is changed from 0 to a nominal value for a 2.2 kW induction motor (parameters of the motor will be elaborated on later). It can be seen that h_2 has the minimum value at zero speed. Therefore, the most critical speed, from the robustness point of view, is zero speed. Therefore, Eq. (13) should be solved with $h_2 = 0.7$. Solving Eq. (13) by means of the Doyle–Glover algorithm, which was introduced in [26], for the test motor gives the robust gain as $K = 5.1272 + j12.8180$.

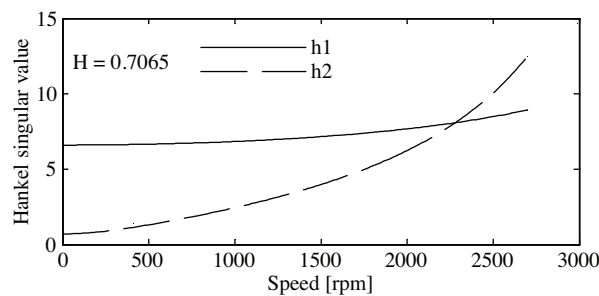


Figure 1. Hankel singular values' variation with speed change.

3. Robust closed loop prediction model

Despite all of the techniques that have been proposed to reinforce the accuracy of the reduced order observer, the estimation error for the speed and flux that are injected into the prediction model can affect the prediction accuracy in sensorless application. In this paper a robust closed loop prediction model is proposed to reduce

the sensitivity of the prediction model to the errors that are being injected from observer.

$$\begin{aligned}\hat{\psi}_s[k+1] &= \hat{\psi}_s[k] - t_s R_s \bar{I}_s + t_s \bar{V}_s + t_s K_1 \operatorname{sgn}(\hat{I}_{sp} - \bar{I}_s) \\ \hat{I}_s[k+1] &= \left\{ \frac{t_s R_r}{\sigma L_s L_r} - j \frac{\hat{\omega}_r t_s}{\sigma L_s} \right\} \hat{\psi}_s[k] + \left\{ \frac{t_s R_s}{\sigma L_s} + \left(1 - \frac{t_s R_r}{\sigma L_r} \right) + j \hat{\omega}_r t_s \right\} \bar{I}_s \\ &\quad + \frac{t_s}{\sigma L_s} \bar{V}_s + t_s K_2 \operatorname{sgn}(\hat{I}_{sp} - \bar{I}_s)\end{aligned}\quad (9)$$

Here, sgn is the sign function and \hat{I}_{sp} is the last predicted current. Note that $\hat{\psi}_s$ and $\hat{\omega}_r$ are estimated flux and speed, respectively, which are received from observer.

By applying the predicted stator flux and stator current, the next step torque can be calculated as follows:

$$\hat{T}(k+1) = \frac{3p}{4} \left\{ \hat{\psi}_{sd}(k+1) \hat{I}_{sq}(k+1) - \hat{\psi}_{sq}(k+1) \hat{I}_{sd}(k+1) \right\}. \quad (10)$$

Since the closed loop prediction model has not been investigated before, calculating the feedback gains will be a new challenge. In order to assign these gains in the closed loop prediction model, the investigations on the gains of the closed loop full order observers are contemplated. In [27], the Lyapunov theory, and in [28], the pole placement method are used. With the pole placement method the dynamic behavior of the model can be tuned. However, the robustness of the model is not considered. Therefore, parameter adaptation was utilized in [29].

In this paper, a combination of the pole placement method and H_∞ theory is proposed to calculate the gains of the closed loop predictive model. The poles are shifted to the left and the amount of shift is calculated by the robustness theory to reduce the sensitivity of the closed loop model to the variation of the resistances and the speed estimation error.

The measured current and the feasible VVs are considered as the inputs of the prediction model. Therefore, the uncertain closed loop prediction model can be explained as follows:

$$\dot{X} = (A' + \Delta A') X + B' U, \quad (11a)$$

$$Y = C' X, \quad (11b)$$

$$X = \begin{bmatrix} \hat{\psi}_s \\ \hat{I}_s \end{bmatrix}, U = \begin{bmatrix} \bar{V}_s \\ \bar{I}_s \end{bmatrix}, Y = \hat{I}_s, \quad (11c)$$

$$A' = \begin{bmatrix} 0 & -R_s + K_1 \\ \frac{R_r}{\sigma L_s L_r} - j \frac{\hat{\omega}_r}{\sigma L_s} & -\frac{R_r}{\sigma L_r} - \frac{R_s}{\sigma L_s} + j \hat{\omega}_r + K_2 \end{bmatrix}, \quad (11d)$$

$$\Delta A' = \begin{bmatrix} 0 & -\Delta R_s \\ \frac{\Delta R_r}{\sigma L_s L_r} - j \frac{\Delta \hat{\omega}_r}{\sigma L_s} & -\frac{\Delta R_r}{\sigma L_r} - \frac{\Delta R_s}{\sigma L_s} + j \Delta \hat{\omega}_r \end{bmatrix}, \quad (11e)$$

$$B' = \begin{bmatrix} 1 & -K_1 \\ \frac{1}{\sigma L_s} & -K_2 \end{bmatrix} C' = [0 \quad 1], \quad (11f)$$

where ΔR_s and ΔR_r are the errors for the stator and rotor resistances, and $\Delta \hat{\omega}_r$ is the speed estimation error.

The model poles can be shifted to the left by feedback gains [30,31]. This method guarantees that the poles of the model remain in the stable region by the speed variation.

For pole shifting, by the amount of K_{sh} , feedback gains are calculated as below:

$$k_{11} = [K_{sh}^2 R_s \sigma a_s a_r + K_{sh} R_s \sigma a_s a_r (a_s + a_r) + K_{sh} \omega^2 R_s a_s] / f, \tag{12a}$$

$$k_{12} = [a_s \omega (K_{sh}^2 R_s + K_{sh} R_s (a_s + a_r)) - K_{sh} R_s \sigma a_s a_r \omega] / f, \tag{12b}$$

$$k_{21} = 2 K_{sh}, \tag{12c}$$

$$k_{22} = 0, \tag{12d}$$

where

$$a_s = \frac{R_s}{\sigma L_s}, \quad a_r = \frac{R_r}{\sigma L_r}, \tag{12e}$$

$$f = R_s^2 \sigma^2 a_s^2 a_r^2 + \omega^2 a_s^2. \tag{12f}$$

However, the variation of the poles in the case of the parameter estimation error or the speed estimation error is not considered. Therefore, the robustness of the method is not guaranteed. In order to show the effect of the stator and rotor resistances' uncertainties, Figure 2 shows the relocation of the shifted closed loop poles after 100% variation of the stator and rotor resistances simultaneously.

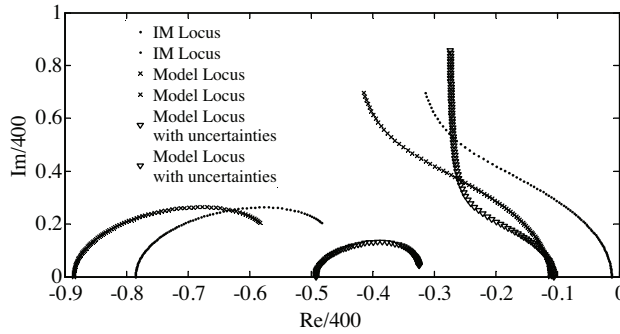


Figure 2. Root locus of model.

In this paper, the shifting amount is calculated via the H_∞ method to achieve the minimum sensitivity of the closed loop system to the uncertainties. For this purpose, K_{sh} should satisfy the following equation [26].

$$\min_{K_{sh}} \left\| C' (sI - A')^{-1} B' \right\|_\infty \tag{13}$$

Since the maximum values for the errors of the stator and rotor resistances, and the estimated speed error, can be forecasted, the suboptimal solution can be replaced instead of Eq. (13):

$$\left\| C' (sI - A')^{-1} B' \right\|_\infty < \frac{1}{\|\Delta A'\|_\infty}. \tag{14}$$

In this paper, the maximum error for the stator and rotor resistances is assumed to be 100% and the maximum of the speed estimation error is set to 50%.

Considering Eq. (11) and Eq. (12) it is clear that the solution of Eq. (14) depends on the value of the speed. Trying to solve Eq. (14) indicates that it does not have any solution at speeds that are lower than 60 rpm (2% of nominal synchronous speed). The minimum pole shift that satisfies Eq. (7) is $K_{sh} = 367.02$ at the aforementioned speed. In order to be sure that this amount of the pole shifting satisfies Eq. (14) at higher speeds, Figure 3 shows the infinity norm of the closed loop model at different speeds. It can be seen that the infinity norm decreases when the speed increases.

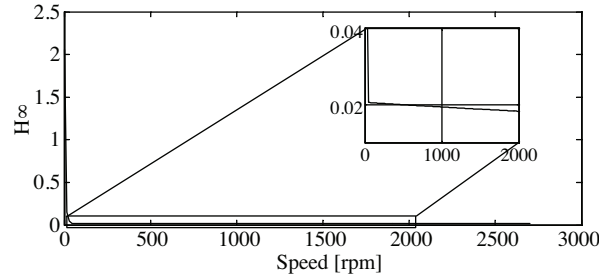


Figure 3. Variation of infinity norms of the closed loop model at various speeds.

4. Predictive torque control method

When the next torque and stator flux are predicted without using the speed sensor, the sensorless PTC method can be implemented. The predicted torque and stator flux are placed in the following cost function. This is a criterion for the minimum control error.

$$J_n = \frac{1}{2} \left(\left| \hat{T}_n(k+1) - T^* \right|^2 + Q \left| \left| \hat{\psi}_{sn}(k+1) \right|^2 - \left| \bar{\psi}_s^* \right|^2 \right|^2 \right) \quad (15)$$

$$n = 1, 2, \dots, 7$$

Here, $\hat{T}_n(k+1)$ and $\hat{\psi}_{sn}(k+1)$ are the predicted torque and stator flux, respectively, which are calculated by means of a proposed prediction model considering the application of the n th voltage vector. T^* and $|\bar{\psi}_s^*|$ are the torque and flux references, respectively. Q is a weighting factor that determines the importance of the flux control compared to the torque control.

In this paper, FCS-MPC is used for the cost function minimization. Therefore, all 7 possible VVs are examined in the cost function and the best application is selected.

Combining the proposed sensorless predictive model and the sensorless observer leads to sensorless PTC. Figure 4 shows the whole block diagram for the sensorless predictive torque control method.

5. Results

In order to verify the proposed sensorless predictive method, the simulation and experimental results are presented. The VVs are exerted by a 2-level inverter. The Table shows the specification of the experimental setup. The simulations are performed with the model of the experimental system. The control interval duration is set to 100 μ s.

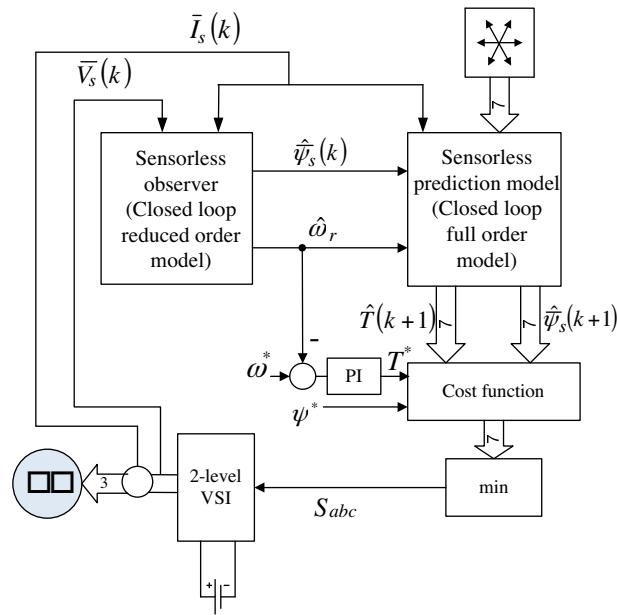


Figure 4. Sensorless FCS-MPC block diagram.

Table. System specifications.

Induction motor	
$P_n = 2.2$ [kW]	$R_s = 2.65$ [Ω]
$V_n = 220$ [V]	$R_r = 2.24$ [Ω]
$I_n = 4.61$ [A]	$L_s = 301$ [mH]
$\omega_n = 2772$ [rpm]	$L_r = 301$ [mH]
$P = 1$	$L_m = 291$ [mH]
$T_n = 7.57$ [Nm]	$f_{sn} = 50$ [Hz]
Inverter	
$V_{dc} = 580$ [V]	$I_n = 25$ [A]
IGBT nominal voltage = 1200 [V]	Control interval = 100 [μ s]
Controlling hardware (industrial PC)	
CPU = INTEL Pentium	Clock frequency = 600 MHz

5.1. Simulation results

The following conditions are considered for simulations. Note that when the effect of a special uncertainty is being investigated, extra error will be considered. The amount of the uncertainty will be determined in those conditions.

1. 5% error for the stator resistances.
2. 5% error for the rotor resistances.
3. 0.1% offset voltage from the measured currents.
4. 1 V threshold voltage for the switches.
5. The friction factor for the whole system (fans and internal friction) is assumed to be $0.02 \text{ Nm s rad}^{-1}$.

Figure 5 shows the transient response of the speed step for the proposed sensorless PTC. The accuracy of the method can be seen here. In order to investigate the robustness of the proposed method against the stator and rotor resistances' variation, these resistances are varied simultaneously and the results are shown in Figure 6. The speed is kept low for studying the most sensitive region. It can be seen that when both observer and prediction models are open loop, the method keeps its robustness up to 18% error for the stator and rotor resistances. If the closed loop models are used but the feedback gains are assigned by the pole shifting method, the method will be robust until 22% error, and when the robust gains assignment is used it keeps its robustness up to 38% error.

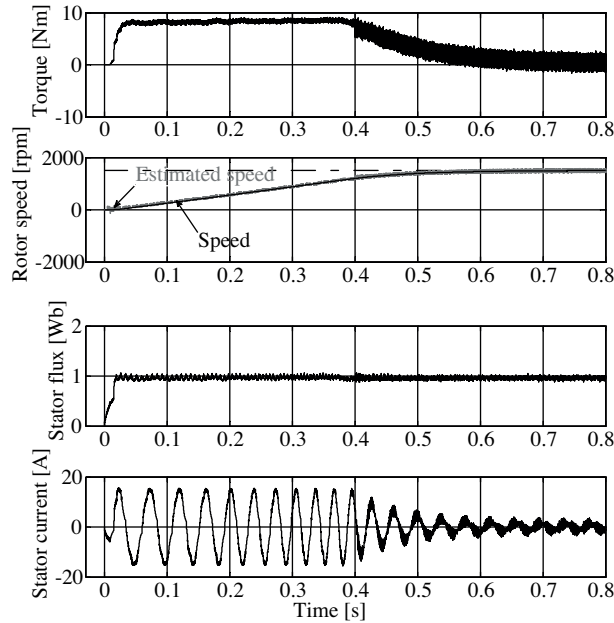


Figure 5. Speed step performance of proposed sensorless PTC: simulation results.

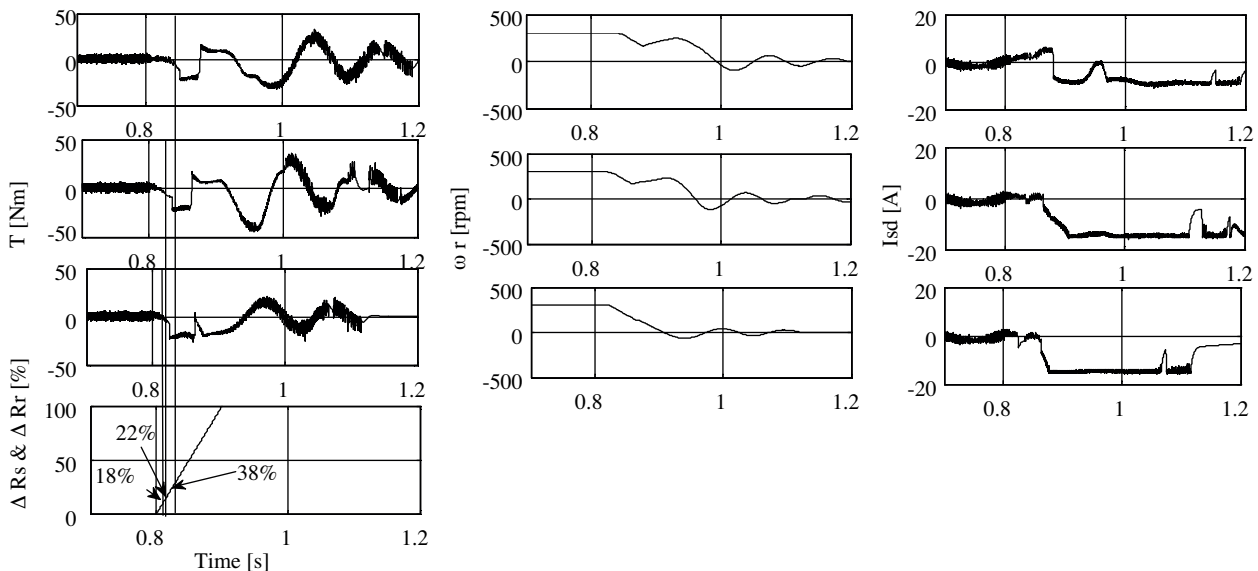


Figure 6. Robustness testing of proposed sensorless PTC against stator and rotor resistance variation: simulation results.

One of the most serious uncertainties that affect the reduced order observer is the offset of the current measurement. In Figure 7 this uncertainty is investigated. Here, 0.75 A is considered for the offset of the current measurement. It is depicted that if both observer and prediction models are closed loop and robust, the oscillations will be reduced compared to the pole shifting closed loop models.

Figure 8 shows the low speed performance of the sensorless PTC with 3 strategies. It can be seen that at 200 rpm (6.6%) when the robust closed loop method is used, the method is robust. When it switches to the pole shifting closed loop method, despite some oscillations, the robustness is still kept. However, it is unstable when the open loop method is applied.

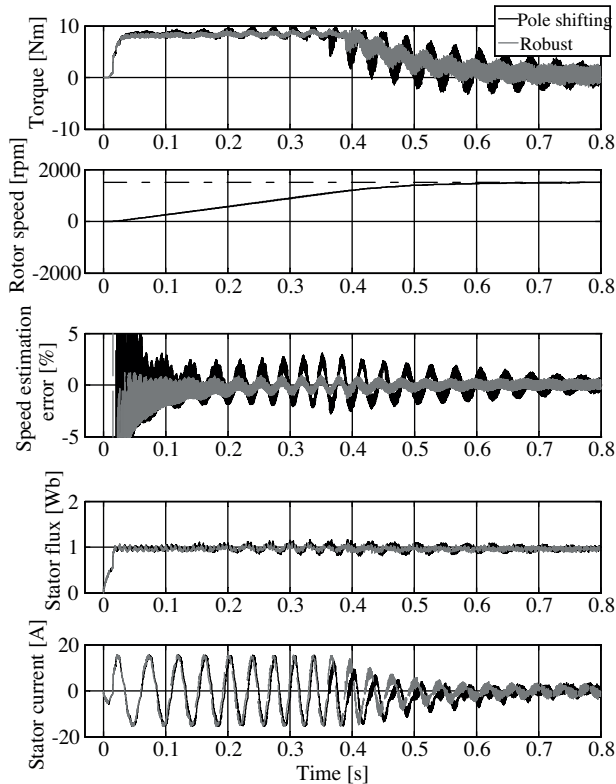


Figure 7. Performance of proposed sensorless under offset condition: simulation results.

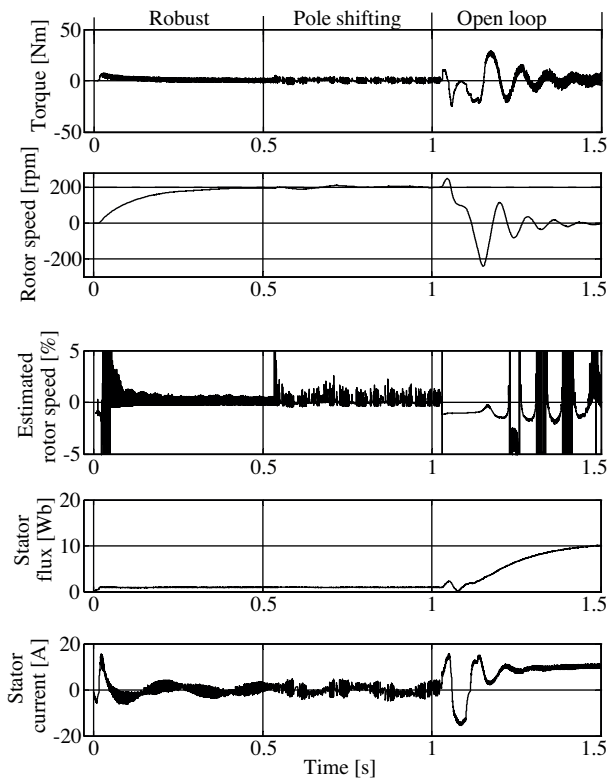


Figure 8. Low speed performance of sensorless PTC: simulation results.

5.2. Experimental results

Figure 9 shows the experimental setup. An industrial PC, which includes a Pentium processor, is used. The dead-time for the inverter is set to 2.5 μ s. The integrated power module PM25RSB120 is used for the 2-level voltage source inverter.

In order to have a short time delay and also avoid the measurement noise, the switching is done in the middle of the control interval. The sequence of the actions in every control interval is as follows:

1. Running the specified timer.
2. Taking the measured samples.
3. Performing all computations of the algorithm.
4. If the timer's value has passed the prescribed point, applying the selected VV and setting the timer's value to zero.

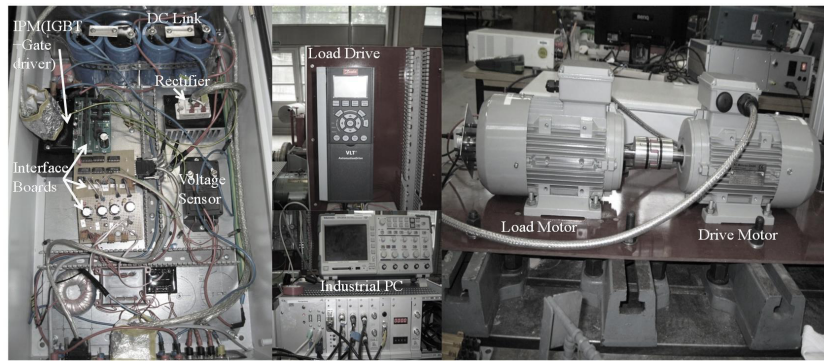


Figure 9. Experimental setup.

In this paper, the switching instant is set to 25% of the control interval. That means the delay time will be 25 μ s. If the computations take more than this time, the switching will take place after the finishing of the computations. Since the delay time is less than a complete control interval, there is no need for delay time compensation.

Figure 10 shows the positive and negative speed step responses of the proposed sensorless PTC method. In Figure 11 the low speed performance of the proposed sensorless PTC method is depicted. It can be seen that the method is stable at 220 rpm (7.3%).

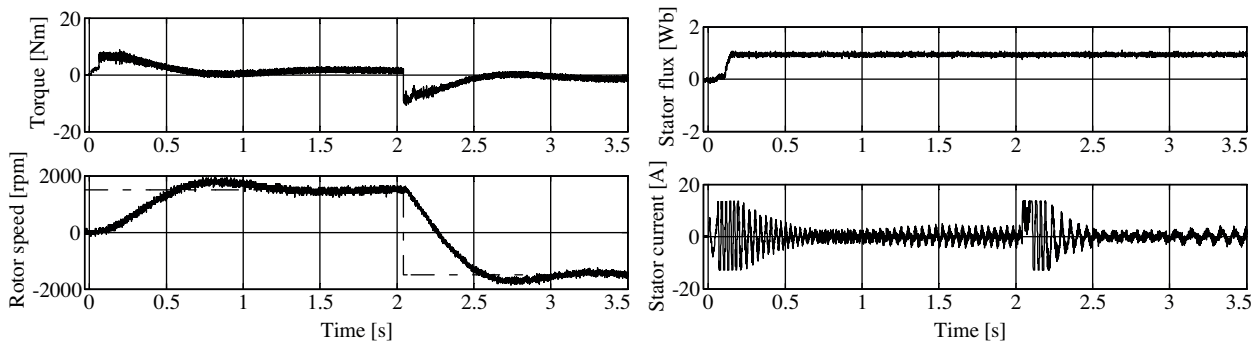


Figure 10. Speed control for proposed sensorless PTC: experimental results.

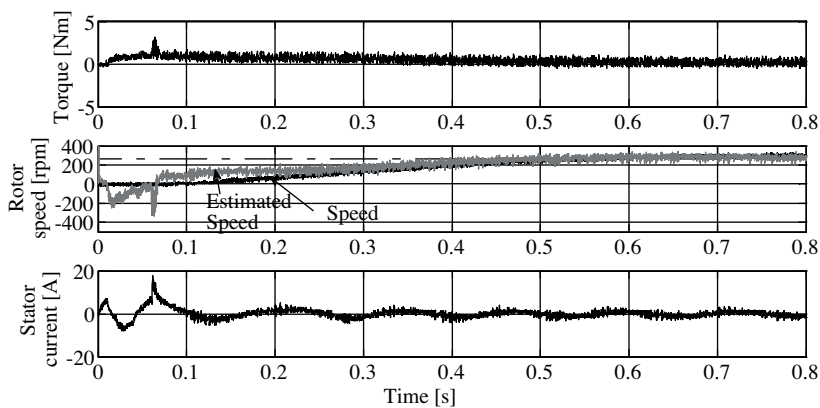


Figure 11. Low speed performance of proposed sensorless PTC: experimental results.

In order to investigate the transient response to the torque step under the load condition, Figure 12 shows the transient torque response when the load torque is 3 Nm.

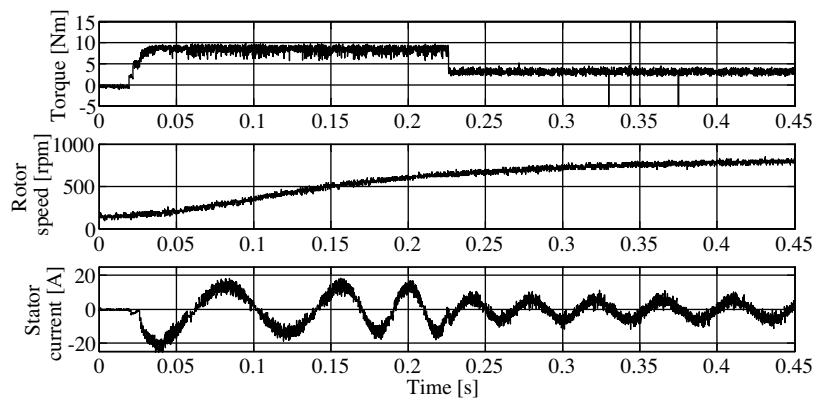


Figure 12. Torque step response of proposed sensorless PTC: experimental results.

6. Conclusion

A novel robust sensorless PTC method with a reduced order observer was proposed. A closed loop sliding mode reduced order observer was proposed and used for the speed and flux estimation. The feedback gains of this observer were assigned with the robustness H_∞ analysis. The outputs of the observer were used in a proposed closed loop sliding mode full order prediction model to predict the torque and flux. Using the robust closed loop models for both the observer and prediction models eliminates the need for the speed or the parameter adaptation in the observer or the prediction model.

The proposed method was verified by the simulation and experimental results. The results show that the method is robust in the low speed range up to 7.3%. The method keeps its robustness against the stator and rotor resistances' error up to 38% in a low speed region. The method can compensate 0.75 A offset for the current measurement.

This method can be a better alternative for the DTC method because it has the advantages of DTC and PTC together.

References

- [1] P. Mutschler, E. Flach, "Digital implementation of predictive direct control algorithms for induction motors", IEEE Industry Applications Conference, 33rd IAS Annual Meeting, Vol. 1, pp. 444–451, 1998.
- [2] R. Kennel, A. Linder, "Predictive control of inverter supplied electrical drives", IEEE Power Electronics Specialists Conference, Vol. 2, pp. 761–766, 2000.
- [3] E. Flach, R. Hoffmann, P. Mutschler, "Direct mean torque control of an induction motor", European Conference on Power Electronics and Applications, Vol. 3, pp. 672–677, 1997.
- [4] P. Correa, M. Pacas, J. Rodriguez, "Predictive torque control for inverter-fed induction machines", IEEE Transactions on Industrial Electronics, Vol. 54, pp. 1073–1079, 2007.
- [5] A. Linder, R. Kanchan, R. Kennel, P. Stolze, Model-Based Predictive Control of Electric Drives, Cuvillier Verlag, Munich, 2010.
- [6] R. Kennel, A. Linder, M. Linke, "Generalized predictive control (GPC)-ready for use in drive applications?", IEEE 32nd Annual Power Electronics Specialists Conference, Vol. 4, pp. 1839–1844, 2001.
- [7] K.S. Low, H. Zhuang, "Robust model predictive control and observer for direct drive applications", IEEE Transactions on Power Electronics, Vol. 15, pp. 1018–1028, 2000.
- [8] S.A. Davari, D.A. Khaburi, R. Kennel, "An improved FCS-MPC algorithm for induction motor with imposed optimized weighting factor", IEEE Transactions on Power Electronics, Vol. 27, pp. 1540–1551, 2012.

- [9] R. Vargas, U. Ammann, J. Rodriguez, "Predictive approach to increase efficiency and reduce switching losses on matrix converters," *IEEE Transactions on Power Electronics*, Vol. 24, pp. 894–902, 2009.
- [10] T. Laczynski, A. Mertens, "Predictive stator current control for medium voltage drives with LC filters", *IEEE Transactions on Power Electronics*, Vol. 24, pp. 2427–2435, 2009.
- [11] S.A. Davari, E. Hasankhan, D.A. Khaburi, "A comparative study of DTC-SVM with three-level inverter and an improved predictive torque control using two-level inverter", *IEEE 2nd Annual Power Electronics, Drive Systems and Technologies Conference*, pp. 379–384, 2011.
- [12] R. Vargas, U. Ammann, B. Hudoffsky, J. Rodriguez, P. Wheeler, "Predictive torque control of an induction machine fed by a matrix converter with reactive input power control", *IEEE Transactions on Power Electronics*, Vol. 25, pp. 1426–1438, 2010.
- [13] S.A. Davari, D.A. Khaburi, "Sensorless predictive torque control by means of sliding mode observer", *IEEE 2nd International Power and Energy Conference*, pp. 707–711, 2008.
- [14] C. Lascu, I. Boldea, F. Blaabjerg, "Direct torque control of sensorless induction motor drives: a sliding-mode approach", *IEEE Transactions on Industrial Applications*, Vol. 40, pp. 582–590, 2004.
- [15] P. Landsmann, D. Paulus, P. Stolze, R. Kennel, "Saliency based encoderless predictive torque control without signal injection", *IEEE International Power Electronics Conference*, pp. 3029–3034, 2010.
- [16] P. Landsmann, D. Paulus, P. Stolze, R. Kennel, "Reducing the parameter dependency of encoderless predictive torque control for reluctance machines", *IEEE First Symposium on Sensorless Control for Electrical Drives*, pp. 93–99, 2010.
- [17] H. Abu-Rub, J. Guzinski, J. Rodriguez, R. Kennel, P. Cortés, "Predictive current controller for sensorless induction motor drive", *IEEE International Conference on Industrial Technology*, pp. 1845–1850, 2010.
- [18] S. Mariethoz, A. Domahidi, M. Morari, "Sensorless explicit model predictive control of permanent magnet synchronous motors", *IEEE International Conference on Electric Machines and Drives*, pp. 1250–1257, 2009.
- [19] T.H. Liu, C.L. Chen, J.L. Chen, "Implementation of a predictive controller for a sensorless IPMSM drive system", *IEEE International Conference on Industrial Technology*, pp. 165–170, 2011.
- [20] S.A. Davari, D.A. Khaburi, "Sensorless predictive torque control of induction motor by means of reduced order observer", *IEEE 2nd Annual Power Electronics, Drive Systems and Technologies Conference*, pp. 484–488, 2011.
- [21] E.E. Özsoy, M. Gökaşan, S. Bogosyan, "Simultaneous rotor and stator resistance estimation of squirrel cage induction machine with a single extended Kalman filter", *Turkish Journal of Electronic Engineering & Computer Science*, Vol. 18, pp. 853–863, 2010.
- [22] S. Partal, İ. Şenol, A.F. Bakan, K.N. Bekiroğlu, "Online speed control of a brushless AC servomotor based on artificial neural networks", *Turkish Journal of Electronic Engineering & Computer. Science.*, Vol. 19, pp. 373–383, 2011.
- [23] Ö. Göksu, A.M. Hava, "Experimental investigation of shaft transducerless speed and position control of ac induction and interior permanent magnet motors", *Turkish Journal of Electronic Engineering & Computer Science*, Vol. 18, pp. 865–882, 2010.
- [24] M.G. Aydeniz, İ. Şenol, "A Luenberger-sliding mode observer with rotor time constant parameter estimation in induction motor drives", *Turkish Journal of Electronic Engineering & Computer Science*, Vol. 19, pp. 901–912, 2011.
- [25] J. Holtz, J. Quan, "Drift- and parameter-compensated flux estimator for persistent zero-stator-frequency operation of sensorless-controlled induction motors", *IEEE Transactions on Industrial Applications*, Vol. 39, pp. 1052–1060, 2003.
- [26] D. W. Gu, P.H. Petkov, M.M. Konstantinov, *Robust Control Design with MATLAB*, London, Springer, 2005.
- [27] C. Lascu, G.D. Andreescu, "Sliding-mode observer and improved integrator with DC-offset compensation for flux estimation in sensorless-controlled induction motors", *IEEE Transactions on Industrial Electronics*, Vol. 53, pp. 785–794, 2006.

- [28] M. Tursini, R. Petrella, F. Parasiliti, “Adaptive sliding-mode observer for speed-sensorless control of induction motors”, *IEEE Transaction on Industrial Applications*, Vol. 36, pp. 1380–1387, 2000.
- [29] C. Lascu, I. Boldea, F. Blaabjerg, “Variable-structure direct torque control—a class of fast and robust controllers for induction machine drives”, *IEEE Transactions on Industrial Electronics*, Vol. 51, pp. 785–792, 2004.
- [30] C. Lascu, I. Boldea, F. Blaabjerg, “Comparative study of adaptive and inherently sensorless observers for variable-speed induction-motor drives”, *IEEE Transactions on Industrial Electronics*, Vol. 53, pp. 57–65, 2006.
- [31] J. Maes, J.A. Melkebeek, “Speed-sensorless direct torque control of induction motors using an adaptive flux observer”, *IEEE Transactions on Industrial Applications*, Vol. 36, pp. 778–785, 2000.